Guided ion beam studies of the reactions of Cr_n^+ ($n = 2 - 18$) with O_2: Chromium cluster oxide and dioxide bond energies

James B. Griffin and P. B. Armentrout
Department of Chemistry, University of Utah, Salt Lake City, Utah 84112

The kinetic energy dependence of the reactions of Cr_n^+ ($n = 2 - 18$) with O_2 are studied in a guided ion beam mass spectrometer. A variety of $Cr_mO_2^+$, Cr_mO^+, and Cr_m^+ product ions, where $m \leqslant n$, are observed, with the dioxide cluster ions dominating the products for all larger reactant cluster ions. Reaction efficiencies are near unity for all but the smallest clusters. The energy dependence of the product cross sections is analyzed in several different ways to determine thermochemistry for both the first and second oxygen atom binding to chromium cluster ions. These values show little dependence on cluster size for clusters larger than three atoms. The trends in this thermochemistry are discussed and compared to bulk phase oxidation values. © *1998 American Institute of Physics.* [S0021-9606(98)01919-9]

I. INTRODUCTION

Oxidation of transition metals is a subject of considerable interest because of its importance in corrosion. It has long been known that an alloy of iron and chromium displays a resistance to corrosion and is given the name ''stainless'' steel. There are various types of alloys that include carbon for hardness and nickel. The chromium atoms in stainless steel are known to play a sacrificial role in the oxidation process. The chromium atoms are selectively oxidized at the metal surface to form a Cr_2O_3 (passivated) surface.[1] This surface forms rapidly as clean stainless is exposed to atmospheric oxygen. This would seem to indicate that the bulk chromium oxide bond energy is stronger than that of bulk iron oxide although the monomer Cr–O bond (4.51 eV)[2] is only slightly stonger than the Fe–O bond (4.23 eV).[3] Providing insight into the mechanisms and energetics of this oxidation process compared to that of iron may therefore be of technological value, as well as of fundamental interest.

Several studies of gas phase chromium oxides have been reported in the literature.[2,4-7] Recently, the photoelectron spectrum of CrO^- was studied and the electron affinity and excited states of the CrO neutral were reported.[4] Larger chromium oxide anions have also been observed and their relative stabilities assessed.[5] Other thermodynamic properties of neutral CrO, including its bond energy and ionization energy, have also been determined.[2,6] Reactions of laser ablated chromium atoms reacting with oxygen have recently been studied using Fourier-transform infrared (FTIR).[7] Here, CrO and OCrO are formed and deposited into a solid argon matrix. Association of reagents and primary products in the matrix led to formation of higher order chromium oxides. Infrared absorption frequencies were reported and structures were proposed.

The oxidation of neutral chromium clusters has been studied in a fast flow reactor where the products are monitored by ionization and time of flight mass spectrometry.[8] In the experimental setup of Nieman *et al.*, the oxygen reactant was admitted to the flow reactor downstream of the cluster formation region. They found that the initial stages of oxidation favored formation of the cluster dioxides, Cr_nO_2, with little or no increase in the intensity of Cr_nO species. The efficiencies of these reactions were estimated to be close to unity. As the O_2 pressure was increased, they found that the dominant products formed were Cr_nO_m, where n is slightly larger than m. For the clusters $n > 10$, it was found that the ratio m/n quickly attains a constant value of about 1.28.[8]

There have been many studies of the oxidation of chromium surfaces.[9] This work establishes that the mechanism of chromium oxidation is dissociative chemisorption with the formation of disordered Cr_2O_3 lattices which may be annealed to organized crystals. Little thermochemical information is available from these sources because the surfaces reconstruct upon oxidation, thereby making quantification of the energetics difficult. Calorimetry studies on chromium films find that the desorption of molecular oxygen from chromium oxide surfaces requires 7.6 ± 0.3 eV.[10]

In the present work, we examine the reactions of chromium cluster cations, Cr_n^+ ($n = 2 - 18$) with oxygen. This extends our growing database of studies on transition metal reactivities which now includes Fe_n^+, V_n^+, and Cr_n^+ with D_2, O_2, and CO_2.[11-15] In contrast to the flow reactor studies that examine reactions only at thermal energies, the kinetic energy dependence of these reactions over a wide range is studied here using guided ion beam mass spectrometry. Qualitatively, our reactivity results at thermal energies parallel the observations for neutral chromium clusters.[8] However, by analyzing the kinetic energy dependence of these processes, we are able to obtain quantitative data regarding the thermodynamics of the oxidation reactions. The trends in this information are discussed in some detail and compared with bulk phase thermochemistry. A key to this analysis is the availability of quantitative thermochemistry regarding the stability of the bare chromium clusters, previously measured in our laboratories.[16]

II. EXPERIMENT

The ion beam apparatus and experimental techniques used in this work have been described in detail elsewhere.[17] Briefly, a copper vapor laser (Oxford ACL-35, 511 and 578 nm, 6–8 kHz repetition rate, 3–4 mJ/pulse) is tightly focused onto a rotating and translating chromium plated iron rod. The plasma thus created is entrained in a continuous flow of helium at a flow rate between 4000 and 6000 sccm. The helium is passed through a liquid N_2 cooled molecular sieve trap to remove impurities. Clustering of the chromium atoms and ions occurs in a 2 mm diameter, 6.4 cm long channel that immediately follows the target. An average ion undergoes approximately 10^5 collisions with He in this channel, a number that should be sufficient to equilibrate the ions to the temperature of the He carrier gas. The gas mixture expands from the clustering channel into the source chamber in a mild supersonic expansion that further cools the internal modes of the clusters. Chromium cluster ions thus created are therefore believed to be fully thermalized and may be cooler. The region between the vaporization block and the skimmer is kept field free and the focusing lenses in the two differential regions that follow are also kept at low potentials so that collisional reheating of the cluster ions is minimized.

The chromium cluster ions are extracted from the source, focused into a magnetic sector for mass analysis, decelerated to a desired kinetic energy, and focused into a radio frequency (rf) octopole ion beam guide.[18] Reactions take place within the octopole where the neutral gas (O_2) is introduced. The octopole beam guide utilizes rf electric fields to create a potential well that traps ions in the transverse direction without affecting their axial energy. Product and unreacted cluster ions drift out of the collision chamber to the end of the octopole, where they are extracted and focused into a quadrupole mass filter for mass analysis. The quadrupole has a mass limit of ~ 1100 amu such that chromium cluster reaction products up to $Cr_{18}O_2^+$ can be studied. Finally, ions are detected by a 27 kV conversion dynode, secondary electron scintillation ion counter,[19] and the signal is processed using standard counting techniques. Conversion of detected ion intensities into reaction cross sections is treated as discussed previously.[20] Absolute cross sections measured in our laboratory have an uncertainty estimated as $\pm 30\%$ and relative uncertanties of $\pm 5\%$.

Laboratory ion energies (lab) are converted to energies in the center-of-mass frame (CM) by using $E(CM) = E(lab)\, M/(M+m)$, where m is the cluster ion mass and M is the mass of dioxygen (32.00 amu). Unless stated otherwise, all energies quoted in this paper correspond to the CM frame. The absolute energy scale and the corresponding full width at half maximum (FWHM) of the ion kinetic energy distribution are determined by using the octopole ion beam guide as a retarding energy analyzer. The uncertainty in the absolute energy scale is ± 0.05 eV (lab) and the widths range from 0.7 to 2.3 eV.

III. RESULTS

Guided ion beam studies from our laboratory for the reaction of Cr^+ with O_2 have been reported previously[2] and

TABLE I. Known thermochemical data (eV).[a]

	D_0	IE
Cr	$\cdots$	6.766^{b}
Cr_2	$1.43\ (0.05)^{c}$	$6.89\ (0.08)^{c}$
Cr_2^+	$1.30\ (0.06)^{c}$	$\cdots$
CrO	$4.51\ (0.15)^{d}$	$7.56\ (0.19)^{d}$
Cr^+–O	$3.72\ (0.12)^{d}$	$\cdots$
OCr–O	$5.27\ (0.61)^{e}$	$10.3\ (0.5)^{f}$
OCr^+–O	$2.5\ (0.8)^{g}$	$\cdots$
O_2	$5.116\ (0.002)^{e}$	12.071^{e}
O	$\cdots$	13.619^{e}

[a]Uncertainties given in parentheses.
[b]Reference 25.
[c]Reference 34.
[d]Reference 2.
[e]Reference 22.
[f]Reference 26.
[g]Calculated from $D(OCr–O)+IE(CrO)–IE(CrO_2)$.

are included in this discussion to lead into the trends for the larger clusters. In all systems, the reactions were carried out from thermal energies to 10 eV in the center-of-mass frame. As a general nomenclature, we will refer to $Cr_mO_2^+$ products as "cluster dioxides," Cr_mO^+ products as "cluster monoxides," and Cr_m^+ products as "cluster fragments," where $m \le n$ for reaction of Cr_n^+. A complete set of figures for all Cr_n^+ clusters ($n = 2$–18) reacting with O_2 can be obtained from Ref. 21. Thermochemistry used to determine some of the threshold energies for the smallest clusters is listed in Table I. Throughout the text, thermochemistry for the bare cluster dissociation energies is obtained from Ref. 16.

In all of these systems, there are two difficulties in obtaining reliable data, as discussed previously.[11,12] First, the cross sections shown here have been corrected for overlap of adjacent mass peaks as long as the corrections are unambiguous. Second, the cross sections shown below correspond to products formed only in single reactive collisions. Products formed in secondary reactions with O_2 were identified by examining the pressure dependence of the cross sections.

A. Cr_n^+ ($n=1$ and 2)$+O_2$

Atomic Cr^+ (^6S) ions react with O_2 in only a single endothermic process to form $CrO^+ + O$. The cross section for this reaction rises from a threshold of ~ 1.3 eV and reaches a peak of about 2.4 Å^2 near the neutral bond energy $D(O_2)^{22}$ (Table I), consistent with the onset for dissociation of the product in the overall process $Cr^+ + O_2 \rightarrow Cr^+ + O + O$. Analysis of this energy dependence yields $D_0(Cr^+$–$O) = 3.72 \pm 0.12$ eV.[2]

The addition of a second chromium atom to the reactant ion complicates the process considerably. Although there are only four atoms in the $Cr_2^+ + O_2$ reaction, there are four possible metal containing ionic products, Cr_2O^+, CrO_2^+, CrO^+, and Cr^+, all of which are observed, Fig. 1. Further, there are eight possible reaction *pathways* for this system, (1)–(8). The thermochemistry for these reactions is indicated as the heat of reaction in eV at 0 K and is based on values from Table I, Ref. 16, and the results determined below.
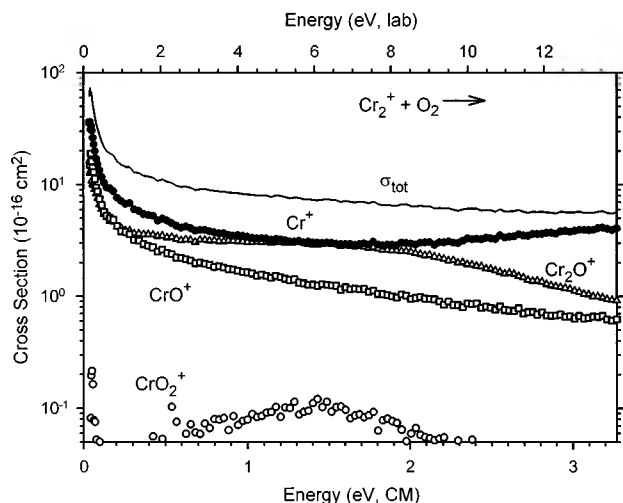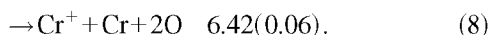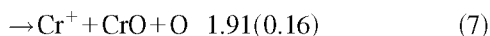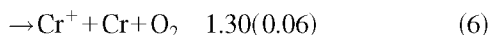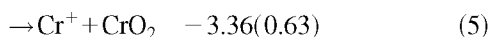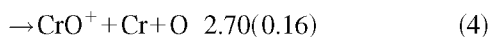
FIG. 1. Cross sections for the reaction of Cr_2^+ with O_2 as a function of collision energy in the center-of-mass (lower x axis) and laboratory (upper x axis) frames.
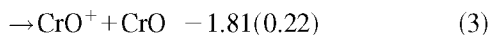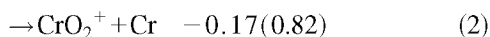

FIG. 2. Cross sections for the reaction of Cr_3^+ with O_2 as a function of collision energy in the center-of-mass (lower x axis) and laboratory (upper x axis) frames.

$$Cr_2^+ + O_2 \quad \rightarrow Cr_2O^+ + O \quad -0.16(0.17) \tag{1}$$

$$\rightarrow CrO_2^+ + Cr \quad -0.17(0.82) \tag{2}$$

$$\rightarrow CrO^+ + CrO \quad -1.81(0.22) \tag{3}$$

$$\rightarrow CrO^+ + Cr + O \quad 2.70(0.16) \tag{4}$$

$$\rightarrow Cr^+ + CrO_2 \quad -3.36(0.63) \tag{5}$$

$$\rightarrow Cr^+ + Cr + O_2 \quad 1.30(0.06) \tag{6}$$

$$\rightarrow Cr^+ + CrO + O \quad 1.91(0.16) \tag{7}$$

$$\rightarrow Cr^+ + Cr + 2O \quad 6.42(0.06). \tag{8}$$

All products have cross sections at low energies that decrease with increasing energy, characteristic of exothermic processes and consistent with reactions (1), (2), (3), and (5). Such behavior can often be quantified by the Langevin–Gioumousis–Stevenson (LGS)[23] formula, $\sigma_{LGS} = \pi e (2\alpha/E)^{1/2}$, where α is the polarizability of O_2 (1.57 Å[3]),[24] e is the charge on the electron, and E is the kinetic energy. We find that the total cross section follows $\sigma_{LGS}/3$ from 0.1 to 1.0 eV, but at thermal energies, the cross section begins at about 0.6 σ_{LGS}.

Although the Cr^+ and CrO^+ cross sections parallel σ_{LGS} below 1 eV, the Cr_2O^+ cross section flattens out above 0.25 eV. Ordinarily this would suggest a new pathway for formation of this ion; however, oxygen atoms are the only neutral product that can correspond to this ion. It seems plausible that a second pathway involving a different electronic state of this product might be involved, but there is insufficient information to evaluate such a possibility further. Above 1.8 eV, the Cr_2O^+ cross section declines, corresponding with an increase in the Cr^+ cross section which indicates that Cr_2O^+ is decomposing to $Cr^+ + CrO$. This is the lowest energy dissociation pathway given the ionization energies IE(Cr) <IE(CrO), Table I. Formation of $CrO_2^+ + Cr$ is the least probable product channel, unlike the larger cluster ions where cluster dioxides are major ionic products. For the

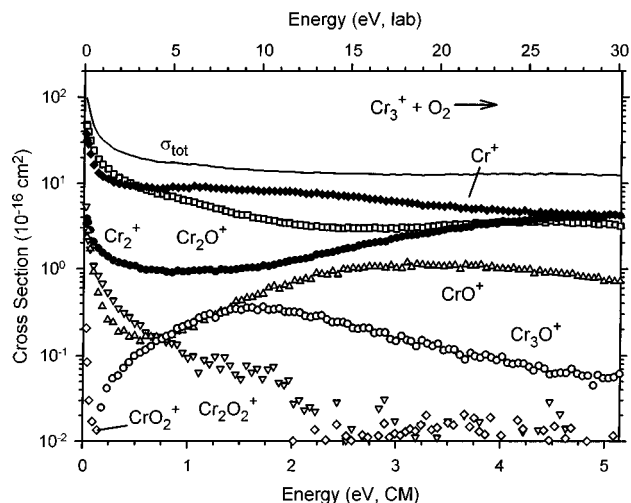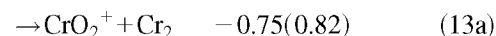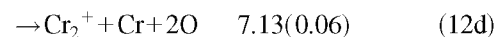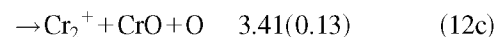dimer reactant, reaction (2) is disfavored compared to reaction (5) because CrO_2 has a much higher ionization energy than Cr (Table I).[25,26]

The dominant product over most of the energy range examined is the Cr^+ fragment, which displays the most complicated energy dependence because there are four possible pathways to form this ion. Reaction (5) is the only pathway to which the exothermic portion of this cross section can be attributed. As noted above, the rise in the Cr^+ cross section is coupled with the decrease in the Cr_2O^+ cross section and can be attributed to reaction (7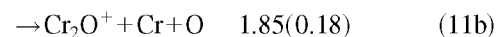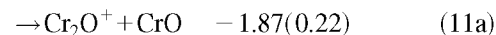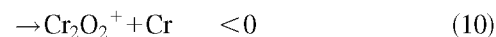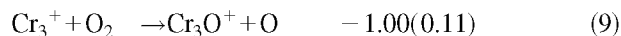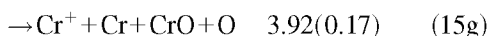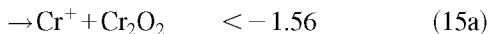). It is possible that reaction (6), simple collision induced dissociation (CID), does contribute to the formation of the Cr^+ product observed. The CID cross section of Cr_2^+ with Xe^{16} has a comparable magnitude to the Cr^+ cross section observed here, but there are no obvious indications that this is a major channel in the present system.

B. $Cr_3^+ + O_2$

In the reaction of the chromium trimer with O_2, there are seven possible reaction products, six of which are observed (all but $Cr_3O_2^+$), Fig. 2. Further, there are now 23 reaction pathways, reactions (9)–(15), that are accessible, but not all of these are observed. Reaction enthalpies at 0 K are based on information from Table I, Ref. 16, and below.

$$Cr_3^+ + O_2 \quad \rightarrow Cr_3O^+ + O \quad -1.00(0.11) \tag{9}$$

$$\rightarrow Cr_2O_2^+ + Cr \quad <0 \tag{10}$$

$$\rightarrow Cr_2O^+ + CrO \quad -1.87(0.22) \tag{11a}$$

$$\rightarrow Cr_2O^+ + Cr + O \quad 1.85(0.18) \tag{11b}$$

$$\rightarrow Cr_2^+ + CrO_2 \quad -2.65(0.63) \tag{12a}$$

$$\rightarrow Cr_2^+ + Cr + O_2 \quad 2.01(0.06) \tag{12b}$$

$$\rightarrow Cr_2^+ + CrO + O \quad 3.41(0.13) \tag{12c}$$

$$\rightarrow Cr_2^+ + Cr + 2O \quad 7.13(0.06) \tag{12d}$$

$$\rightarrow CrO_2^+ + Cr_2 \quad -0.75(0.82) \tag{13a}$$

$\rightarrow CrO_2^+ + 2Cr$	2.18(0.82)	(13b)
$\rightarrow CrO^+ + Cr_2O$	< -2.35	(14a)
$\rightarrow CrO^+ + CrO + Cr$	0.20(0.21)	(14b)
$\rightarrow CrO^+ + Cr_2 + O$	3.27(0.16)	(14c)
$\rightarrow CrO^+ + 2Cr + O$	4.70(0.15)	(14d)
$\rightarrow Cr^+ + Cr_2O_2$	< -1.56	(15a)
$\rightarrow Cr^+ + Cr + CrO_2$	$-1.35(0.63)$	(15b)
$\rightarrow Cr^+ + 2CrO$	$-0.59(0.23)$	(15c)
$\rightarrow Cr^+ + Cr_2O + O$	$< 1.72(0.20)$	(15d)
$\rightarrow Cr^+ + Cr_2 + O_2$	1.88(0.10)	(15e)
$\rightarrow Cr^+ + 2Cr + O_2$	3.31(0.08)	(15f)
$\rightarrow Cr^+ + Cr + CrO + O$	3.92(0.17)	(15g)
$\rightarrow Cr^+ + Cr_2 + 2O$	6.99(0.10)	(15h)
$\rightarrow Cr^+ + 2Cr + 2O$	8.43(0.06).	(15i)

Two cluster dioxide product ions are observed and are assumed to be formed by dissociative chemisorption. The exothermic behavior of the $Cr_2O_2^+$ cross section implies that $D[Cr_2^+-(O)_2]>5.12$ eV. CrO_2^+ is also formed in this system but is the least probable of all products observed. It may be formed by a loss of either two Cr atoms or a Cr dimer from the transient $Cr_3O_2^+$ intermediate. Dimer loss, reaction (13a), makes CrO_2^+ formation exothermic and is reasonable given that dimer loss was observed in CID studies of Cr_3^+.[16] The loss of two Cr atoms probably contributes to the CrO_2^+ cross section at elevated energies.

Among the cluster monoxide products, Fig. 2, the dominant product from thermal energies to about 0.5 eV is Cr_2O^+, which is formed at low energies in reaction (11a). A second feature beginning at about 2.5 eV is due to reaction (11b) and occurs by Cr atom loss from Cr_3O^+. This primary product ion can be formed in only one path, reaction (9). This reaction is exothermic by about 1 eV based on the thermochemistry derived from the reaction of chromium clusters with CO_2.[13]

CrO^+ displays a prominent exothermic feature and an endothermic feature. These must correspond to reactions (14a) and (14b), respectively. The former reaction is suppressed by direct competition with reaction (11a), indicating that $IE(Cr_2O)<IE(CrO)$. Reaction (14b) corresponds to decomposition of the favored Cr_2O^+ product into $CrO^+ + Cr$. Note that this decomposition competes with formation of $Cr^+ + CrO$, reaction (15b). This pathway is thermodynamically favored, consistent with the larger cross section of Cr^+ vs CrO^+.

Metal fragments are also observed as products, Fig. 2. Cr^+ is the dominant product from 0.5 to 5 eV (the highest energy studied for this reaction). Indeed, this product displays a magnitude of 40 Å^2 at thermal energies with a complicated energy dependence including an exothermic feature that can be attributed to reactions (15a)–(15c). Reactions (15d) and (15e) might contribute to the endothermic feature

beginning near 1.2 eV, but it is not possible to assign these features definitively. The exothermic feature in the Cr_2^+ cross section must be a result of reaction (12a) and the second feature starting near 1 eV probably corresponds primarily to reaction (12b), the simple CID process. The magnitude of the Cr_2^+ cross section at these elevated energies is comparable to that observed in CID of Cr_3^+ with Xe.[16] Although contributions from reaction (12c) cannot be excluded definitively, this reaction requires a primary precursor product ion of either Cr_3O^+, which loses CrO, or the Cr_2O^+ product, which loses an oxygen atom. The Cr_3O^+ precursor is too small to contribute significantly to the Cr_2^+ product cross section, and oxygen atom loss from Cr_2O^+ seems improbable as it is the highest energy decomposition pathway for this species.

C. $Cr_4^+ + O_2$

As the number of atoms, n, in the reactant cluster ion increases, the number of products possible for the cluster systems grows as $3n - 1$ and the number of product formation pathways grows much more rapidly. The Cr_4^+ system can produce 11 different products and there are at least 49 possible reaction pathways. As it is laborious to list these pathways for larger clusters, we shall no longer attempt this. Figure 3 represents the product cross sections observed in the reaction of Cr_4^+ with O_2. Ten of the 11 possible products are observed (all but $Cr_4O_2^+$) and most of the cross sections display a complicated energy dependence. Of the cluster dioxide products, Fig. 3(a), the $Cr_3O_2^+$ product can be formed in only a single pathway, accompanied by atomic Cr. The cross section behaves as an exothermic reaction, declining rapidly with energy. This energy dependence indicates that this product has enough energy to dissociate further at all energies examined. This dissociation must correspond to loss of atomic Cr to form the dominant dioxide product at the lowest energies, $Cr_2O_2^+$, which might also be accompanied by Cr_2. At higher energies, the $Cr_2O_2^+$ dissociates to form $Cr^+ + CrO_2$, the lowest energy decomposition pathway. This overall process is exothermic by 0.31 eV if two chromium atoms are formed. CrO_2^+ is formed inefficiently via an exothermic pathway. As formation of $CrO_2^+ + Cr_2 + Cr$ is endothermic by 1.8 ± 0.8 eV, the neutral product must be Cr_3.

Most of the energy dependence for Cr_3^+ is consistent with the simple CID process which has a threshold of 1.04 ±0.10 eV, such that Cr_3^+ is the dominant ionic product above 3.5 eV. The cross section rises more slowly from threshold compared to the CID studies with Xe, but the magnitude at higher energies is similar.[16] At low energies, there is also a small ($\sim 0.001 \ \sigma_{LGS}$) exothermic cross section that must correspond to concomitant CrO_2 formation. The observation that the exothermic formation of Cr_3^+ exceeds the cross section for CrO_2^+ indicates that $IE(Cr_3)<IE(CrO_2)$. There are many pathways for forming Cr^+ and Cr_2^+, but it is difficult to identify any unambiguously. It seems likely that simple CID (with a threshold of 3.05 ± 0.12 eV) produces the highest energy feature observed in the Cr_2^+ cross section above ~5 eV. The reactions $Cr_2^+ + CrO_2 + Cr$ and $Cr_2^+ + 2CrO$ are exothermic by 1.61 and 0.39 eV, respec-

FIG. 3. Cross sections for the reaction of Cr_4^+ with O_2 as a function of collision energy in the center-of-mass (lower x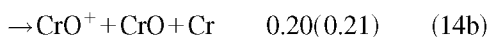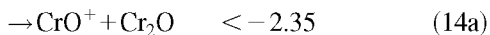 axis) and laboratory (upper x axis) frames. Part a exhibits the cluster dioxide and the cluster fragment products. Part b shows the cluster monoxide products.
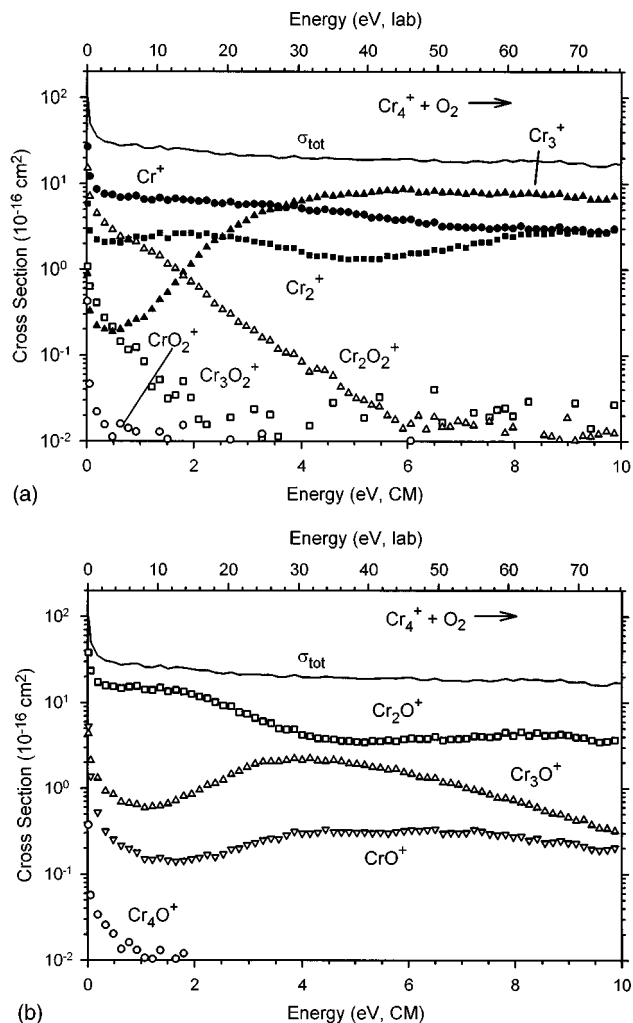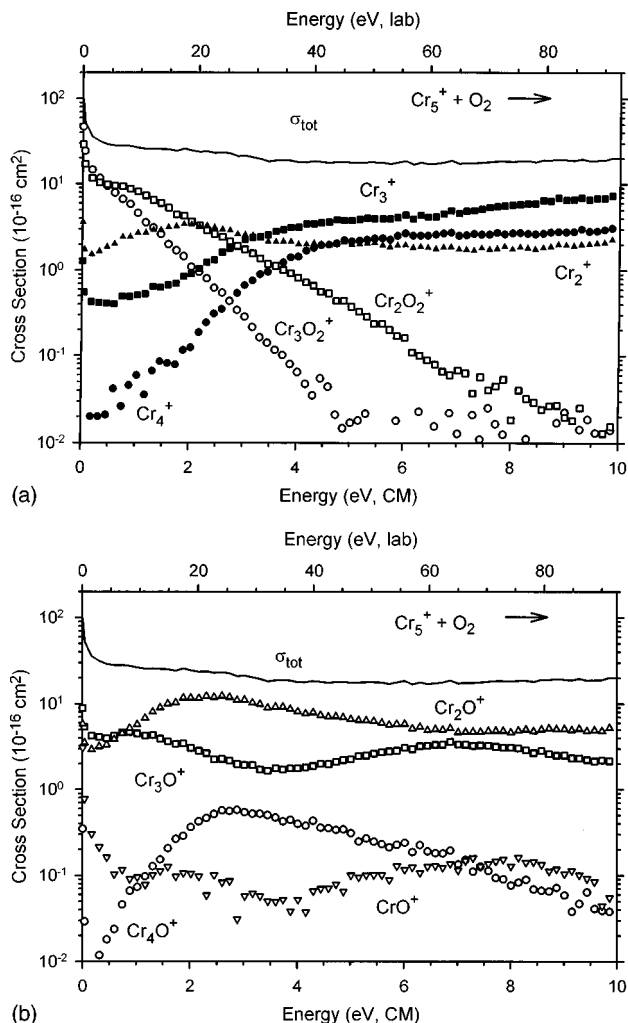
FIG. 4. Cross sections for the reaction of Cr_5^+ with O_2 as a function of collision energy in the center-of-mass (lower x axis) and laboratory (upper x axis) frames. Part a exhibits the cluster dioxide and the cluster fragment products. Part b shows the cluster monoxide products.
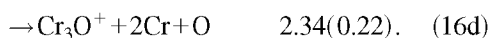
tively, and both could contribute to the cross section observed at lower energies.

Figure 3(b) displays the monoxide products formed in this system. The primary Cr_4O^+ product can only be formed along one exothermic pathway, along with formation of an oxygen atom. The cross section for this product is clearly exothermic and exhibits no indication of the endothermic feature observed in the Cr_nO^+ cross sections for reactions of the dimer and trimer cations. The exothermic feature in the Cr_3O^+ cross section must correspond to formation of a CrO neutral and the endothermic feature to Cr+O formation. The Cr_3O^+ product can then dissociate by loss of a Cr atom at still higher energies, above about 4 eV, where the Cr_3O^+ cross section reaches a maximum and the Cr_2O^+ cross section begins to rise slightly. From this conclusion and the CrO bond energy, the low energy endothermic feature in the Cr_2O^+ cross section can be identified with CrO+Cr neutral products. The cross section for Cr_2O^+ also has an exothermic feature that must therefore correspond to formation of $Cr_2O^+ + Cr_2O$. The cross section for CrO^+ is multifeatured and cannot be analyzed completely because the thermody-

namics of the larger cluster oxide neutrals are not known. At the lowest energies, the CrO^+ and Cr_3O^+ cross sections are roughly equal, which might indicate Cr_3O is formed as a neutral.

D. $Cr_5^+ + O_2$

The product cross sections for this reaction are shown in Fig. 4. Nine of 14 possible product ions are observed. The primary $Cr_4O_2^+ + Cr$ channel is not observed. Instead, the dominant low energy product is $Cr_3O_2^+$, which has a cross section with a magnitude equal to the σ_{LGS} limit. Because $Cr_4O_2^+ + Cr$ is not observed, it seems likely that $Cr_3O_2^+$ is accompanied by a Cr_2 dimer. This is particularly reasonable given that the lowest energy process (by 1.42 eV) for the dissociation of Cr_5^+ is dimer loss.[16] The small exothermic portion of the Cr_2^+ cross section, which probably corresponds to formation of a Cr_3O_2 neutral, also lends some evidence that this is the case. Alternatively, the transient $Cr_5O_2^+$ intermediate can dissociate to form $Cr_2O_2^+$. This cross section appears to have two features; the lowest energy feature

probably corresponds to exothermic Cr_3 formation. Here too, the Cr_3^+ ionic product displays an exothermic portion that probably corresponds to neutral Cr_2O_2 formation, indicating that the charge can go with either product. At slightly elevated energies, the $Cr_2O_2^+$ cross section exceeds that for $Cr_3O_2^+$, which is most likely a result of the decomposition of $Cr_3O_2^+$ by the loss of a Cr atom. This sequence of competitive dissociation pathways can also be observed in the cross sections for these two products in the reaction of the next larger cluster, Cr_6^+.[21] This cross section then begins to decline as the energy increases due to decomposition and competition with other products, primarily the cluster monoxides.

For the cluster monoxide product ions, Fig. 4(b), $Cr_5O^+ + O$ is not stable enough to be observed such that Cr_4O^+ is the largest monoxide product observed. Most of this cross section must correspond to the formation of $Cr + O$ neutrals, as formation of CrO is exothermic by 3.98 ± 0.28 eV. Cr_3O^+ is the dominant monoxide product from the lowest energies to about 0.7 eV. The Cr_3O^+ cross section appears to have three distinct features that can result from reactions (16a)–(16d) (listed in order from most exothermic to most endothermic),

$$Cr_5^+ + O_2 \rightarrow Cr_3O^+ + Cr_2O \qquad < -4.72 \qquad (16a)$$

$$\rightarrow Cr_3O^+ + CrO + Cr \qquad -2.17(0.27) \qquad (16b)$$

$$\rightarrow Cr_3O^+ + Cr_2 + O \qquad 0.91(0.25) \qquad (16c)$$

$$\rightarrow Cr_3O^+ + 2Cr + O \qquad 2.34(0.22). \qquad (16d)$$

The exothermic portion of this cross section is probably due to formation of the Cr_2O in reaction (16a) which might explain the nearly equal magnitude with Cr_2O^+ at the lowest energies. Reaction (16b) is also likely to contribute to the exothermic behavior. The lowest energy endothermic feature is probably from reaction (16c). The third feature beginning near 4 eV is from the dissociation of the primary Cr_4O^+ product by loss of Cr, reaction (16d). The exothermic portion in the Cr_2O^+ cross section is probably due to Cr_3O formation as discussed above. The low energy behavior and correlation between these two products is similar to the dioxides $Cr_2O_2^+$ and $Cr_3O_2^+$. This appears to be because the chromium pentamer cation efficiently fragments into a trimer and dimer. The energy dependence of the CrO^+ cross section is increasingly complicated and contributing pathways cannot be determined unambiguously, as the number of neutral products possible increases and the thermochemistry for many of these is not known.

The cluster fragment ions, Fig. 4(a), have complicated energy dependences. Simple CID, to form Cr_4^+, can begin at 1.04 ± 0.10 eV.[16] This accounts for the major feature in the Cr_4^+ cross section. The Cr_3^+ cross section rises from a threshold that is lower in energy than that of Cr_4^+. This behavior is identical to those observed in the CID studies of Cr_5^+ with Xe, where the lowest energy decomposition is through loss of the neutral dimer. Formation of Cr_3^+ and Cr_2^+ in exothermic processes at low energies was discussed above as they correlate with concomitant formation of oxygenated species. Overall the dioxide products are slightly

FIG. 5. Cross sections for the reaction of Cr_{10}^+ with O_2 as a function of collision energy in the center-of-mass (lower x axis) and laboratory (upper x axis) frames. Part a exhibits the cluster dioxide and the cluster fragment products. Part b shows the cluster monoxide products.
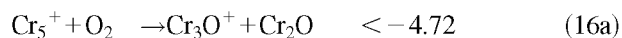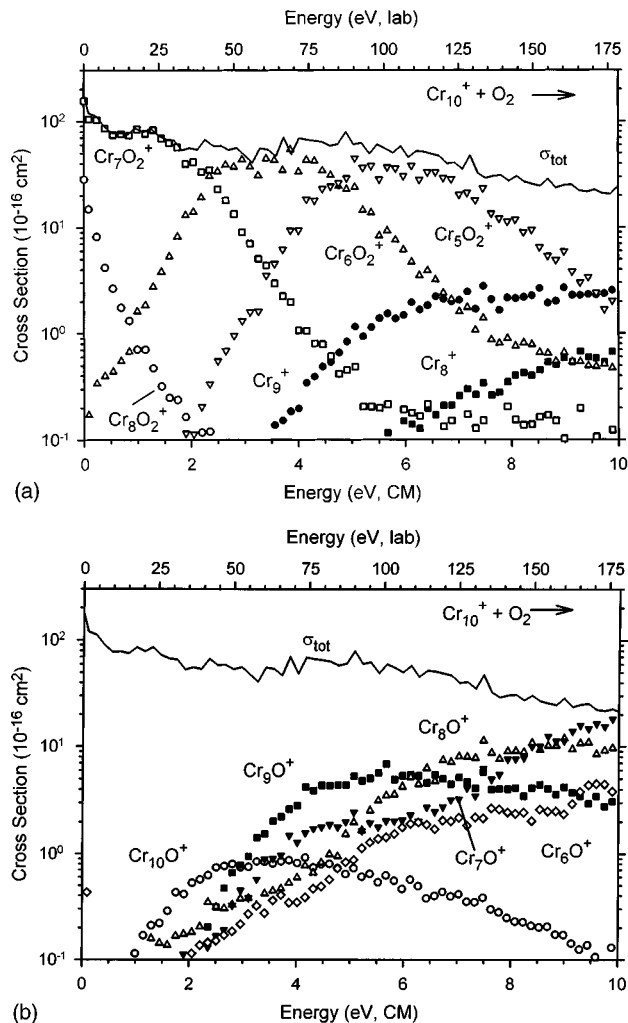
favored over the monoxides and the monoxides over the metal fragments at low energies. At high energies. CID and cluster monoxides dominate the product spectrum.

E. $Cr_n^+ + O_2$ ($n=6-18$)

Although the number of possible reaction products and pathways increases rapidly with increasing reactant cluster size, the reactivity observed actually simplifies and there are strong similarities for different sized clusters. Figures 5 and 6 show results for the reactions of Cr_{10}^+ and Cr_{15}^+ with dioxygen. These two systems are representative of the behavior of all clusters larger than Cr_5^+. The magnitudes of these reaction cross sections at thermal kinetic energies are all comparable to σ_{LGS}.

1. $Cr_mO_2^+$ products

Cluster dioxide ions are the dominant products at low energies [Figs. 5(a) and 6(a)]. As the cluster reactants increase in size, the energy range over which this is true increases from below about 1.25 for Cr_5^+ to about 4 eV for Cr_6^+ to about 8 for Cr_{10}^+ to over 10 eV for Cr_{15}^+. It is clear
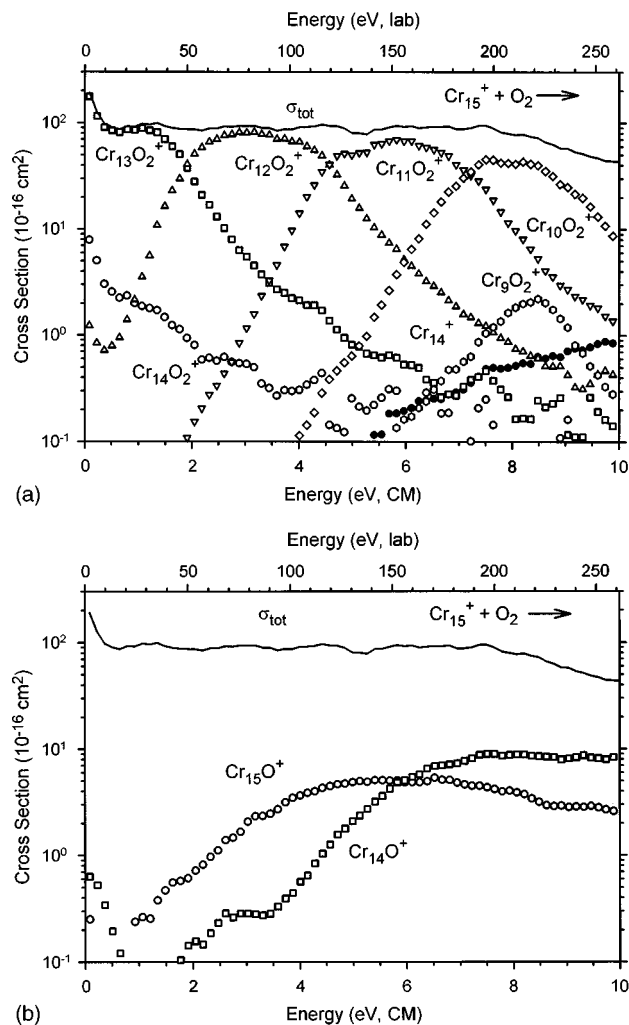
FIG. 6. Cross sections for the reaction of Cr_{15}^+ with O_2 as a function of collision energy in the center-of-mass (lower x axis) and laboratory (upper x axis) frames. Part a exhibits the cluster dioxide and the cluster fragment products. Part b shows the cluster monoxide products.

that the cluster dioxides formed at low energies dissociate by sequential loss of chromium atoms as the energy is increased. This is evident from the observation that the cross sections for $Cr_mO_2^+$ products decline as the $Cr_{m-1}O_2^+$ cross sections rise. If there are any features that might correspond to formation of molecular Cr_{n-m} neutrals, they are negligible within our experimental signal-to-noise ratio. The only exception occurs in the Cr_6^+ system where the cross section for $Cr_2O_2^+$ shows two distinct and reproducible features. One corresponds to formation of 4 Cr and the other to either $Cr_3 + Cr$ or Cr_4. It is also useful to note that because the dissociation process corresponds almost exclusively to $Cr_mO_2^+ \rightarrow Cr_{m-1}O_2^+ + Cr$, this indicates that the ionization energies (IEs) of the larger cluster dioxides must be less than that of atomic Cr, in contrast to the situation for $IE(CrO_2)$.

Although the product distributions are similar for larger clusters, different sized clusters are distinguished by the largest $Cr_mO_2^+$ product (highest m value) observed. While $Cr_{n-3}O_2^+$ dominates for Cr_5^+ to Cr_{11}^+, $Cr_{n-2}O_2^+$ dominates the low energy region in reactions of Cr_{12}^+ to Cr_{17}^+. The $Cr_{n-1}O_2^+$ product cross section is reasonably large for the

Cr_3^+ reaction system, is not observed in the Cr_5^+, Cr_{10}^+, Cr_{11}^+, Cr_{12}^+ systems, and dominates the low energy products at Cr_{18}^+. The $Cr_nO_2^+$ adduct is not observed until Cr_{14}^+ and is a minor product in the Cr_{16}^+ through Cr_{18}^+ systems. The scarcity of the adduct is in marked contrast to the Fe cluster system.[11] This probably results from a combination of the stronger chromium cluster oxygen bond energies and the weaker Cr_n^+-Cr binding energies. These observations are not dependent on the pressure of the O_2 reactant, so that collisional stabilization is not responsible for these products. As documented below, these changes in the dominant $Cr_mO_2^+$ product observed can be attributed to changes in the thermochemistry of the product species.

2. Cr_mO^+ and Cr_m^+ products

For all Cr_n^+ reactants ($n=6-18$), the Cr_nO^+ product cross sections exhibit thresholds in the vicinity of $0.25-1$ eV. As the energy is increased, these products dissociate by sequentially losing chromium atoms [Figs. 5(b) and 6(b)]. We observe that the $Cr_{n-1}O^+$ and $Cr_{n-2}O^+$ cross sections show two features for many cluster sizes. For the $Cr_{n-1}O^+$ product, the lower energy portion must be due to the formation of the CrO neutral. The second feature is a result of the dissociation of the Cr_nO^+ product. For the $Cr_{n-2}O^+$ product, the higher energy feature is clearly due to concomitant formation of 2 Cr+O. The threshold for formation of CrO+Cr should appear about 4.5 eV lower than the higher energy feature; therefore, the low energy endothermic portions observed in Figs. 3(b), 4(b), and 5(b) are probably CrO+Cr formation and the exothermic portions seen in Figs. 3(b) and 4(b) are Cr_2O formation.

For these larger reactant cluster ions ($n=6-18$), the cluster fragment ions are minor products. Typically only the Cr_{n-1}^+ ionic products are observed below 10 eV. These are formed with thresholds largely characteristic of simple CID processes although with magnitudes smaller by about an order of magnitude than observed in the Xe system.[16] Smaller fragments were either not observed or their overall intensity was much less than one percent of all products.

IV. THERMOCHEMISTRY

A. Threshold analysis

The energy dependence of cross sections for endothermic processes in the threshold region is modeled as detailed in our analogous work on iron cluster reactions with O_2,[11] and is outlined in brief here. This procedure uses Eq. (17),[27]

$$\sigma(E) = \sigma_0 \Sigma g_i (E + E_i + E_{rot} - E_0)^N / E, \qquad (17)$$

where σ_0 is an energy independent scaling parameter, N is an adjustable parameter, E is the relative kinetic energy, E_{rot} is the average rotational energy of the cluster ion at 300 K, and E_0 is the threshold for the reaction at 0 K. The summation is over the vibrational states i having energies E_i and populations g_i, where $\Sigma g_i = 1$. Vibrational frequencies for the bare cluster ions are obtained as outlined elsewhere[16,17] and use a Debye model.[28] Equation (17) has been used suc-

TABLE II. Summary of $Cr_n^+-(O)_2$ bond energies (in eV) from several sources.

n	Lower limit[a]	Upper limit[b]	Direct measurement[c]	Relative measurement[d]	Average[e]
1	...	...	...	...	6.3 (0.8)[f]
2	10.51 (0.28)	12.28 (0.35)	11.54 (0.34)	...	11.6 (0.25)
			11.73 (0.38)		
3	10.27 (0.31)	12.87 (0.35)	12.12 (0.41)	12.1 (0.28)	12.1 (0.24)
4	11.83 (0.33)	14.21 (0.38)	13.68 (0.45)	13.5 (0.26)	13.6 (0.26)
5	11.87 (0.28)	14.48 (0.32)	13.68 (0.49)	13.2 (0.32)	13.4 (0.30)
6	12.71 (0.28)	15.17 (0.35)	14.24 (0.57)	13.9 (0.43)	14.1 (0.36)
7	12.57 (0.31)	15.11 (0.35)	14.03 (0.59)	13.7 (0.44)	13.9 (0.37)
8	12.73 (0.30)	15.42 (0.42)	13.71 (0.66)	13.6 (0.46)	13.7 (0.40)
9	10.12 (0.26)	12.81 (0.39)	14.12 (0.51)	13.1 (0.48)	13.6 (0.35)
10	10.35 (0.34)	13.50 (0.47)	12.66 (0.55)	13.1 (0.53)	12.9 (0.38)
11	10.96 (0.44)	14.07 (0.52)	13.36 (0.70)	12.8 (0.60)	13.1 (0.46)
12	11.38 (0.42)	14.21 (0.55)	13.52 (0.57)	12.9 (0.51)	13.2 (0.38)
13	11.06 (0.45)	14.03 (0.58)	13.38 (0.63)	13.2 (0.58)	13.3 (0.43)
14	10.92 (0.52)	13.68 (0.67)	12.81 (0.70)	11.8 (0.68)	12.3 (0.49)
15	10.85 (0.57)	12.87 (0.75)	11.70 (0.78)	11.6 (0.71)	11.7 (0.53)
16	9.90 (0.65)	12.11 (0.79)			11.1 (1.8)[g]
17	9.35 (0.67)	12.27 (0.78)			10.9 (2.2)[g]

[a]Sum of bond energies for loss of three (two for $n>8$) Cr atoms plus $D(O_2)$.
[b]Sum of bond energies for loss of four (three for $n>8$) Cr atoms plus $D(O_2)$.
[c]Calculated from direct threshold measurements listed in Table III using Eq. (18).
[d]Calculated from relative threshold measurements listed in Table III using Eq. (19).
[e]Average of the direct and relative measurements.
[f]Taken from Table I.
[g]Mean of upper and lower limits including uncertainties.

cessfully in reproducing the cross sections of various ion–molecule reactions,[27,29] including those of transition metal cluster ions.[11,12,15–17]

Before comparing the model with all experimental data, several effects are taken into consideration. First, the thermal motion of the target gas and the kinetic energy distribution of the parent ion beam are both convoluted into Eq. (17) as described previously.[30] Second, we extend the range of data analyzed by including a simple statistical model[31] that accounts for the observation that cross sections for both the cluster dioxides and monoxides decline at higher energies because the product dissociates further. Third, low energy "tails" in experimental cross sections, which complicate the data analysis, are treated as detailed in our previous work[11] by ignoring the tails, which will tend to give lower limits for E_0. We believe that the uncertainties listed with the threshold values are sufficiently conservative to include errors introduced by ignoring these isomer tails.

Fourth, we account for the possibility that the processes being modeled occur more slowly than the experimental time window available, $\sim 10^{-4}$ s in our apparatus. This is achieved by incorporating Rice–Ramsperger–Kassel–Marcus (RRKM) theory into Eq. (17) as outlined elsewhere.[32] The implementation of RRKM theory in the present work requires the vibrational frequencies of the oxygenated clusters, the reaction degeneracy, and rotational constants for the bare metal and oxygenated clusters, which are chosen in accord with procedures outlined previously.[11] Here, we chose 473 for the cluster oxygen symmetric stretch, 440 for the asymmetric stretch, and 428 cm^{-1} for the bend. Conservative errors associated with these estimates were evaluated by multiplying and dividing the frequencies by a

factor of 2 and reanalyzing the data. These variations produce differences in the thresholds that are less than 0.02 eV. The choice of the transition state (TS) and its molecular constants parallels those of our previous work[11] and places the TS at the point where the last atom (Cr for all $Cr_xO_2^+$ and $Cr_{n-x}O^+$ products and O for the Cr_nO^+ products) is lost from the oxygenated cluster. The transition state (TS) is assumed to be loose, having molecular constants similar to the dissociated products.[32]

With these various factors included, Eq. (17) can accurately model the experimental cross sections from threshold to 5 eV or more. The parameters, σ_0, N, and E_0 are varied until the model reproduces the data optimally as determined by a nonlinear least squares method. Uncertainties in the listed E_0 values include errors associated with variations in E_0 over the range of N values that adequately reproduce several data sets, variations in the vibrational frequencies of the reactant cluster ion by factors of one-half and two, and the absolute uncertainty in the energy scale.

B. Cluster dioxide bond energies, $Cr_n^+-(O)_2$

1. Qualitative considerations

Before the endothermic reaction cross sections are analyzed, it is worth considering the qualitative characteristics of the cluster dioxide product cross sections to obtain some indication of the magnitude of the cluster dioxide bond energies. One key observation is that the formation of the $Cr_{n-4}O_2^+$ cluster is clearly endothermic (or thermoneutral) for all reactant cluster ions studied. Therefore, an upper limit to the binding energy of two oxygen atoms to the Cr_{n-4}^+ cluster, $D[Cr_{n-4}^+-(O)_2]$, equals $D[Cr_{n-4}^+-Cr]$

TABLE III. Summary of parameters used in Eq. (17) for analysis of $Cr_mO_2^+$ cross sections and relative energy measurements for the dissociation $Cr_mO_2^+ \rightarrow Cr_{m-1}O_2^+ + Cr$.

m	Reactant cluster size, n	σ_0	N	E_0, eV	ΔE measured, eV[a]
2	6	5.3±1.2	2.0±0.2	0.85±0.10	
	7	5.3±13	1.5±0.5	3.31±0.20	
3	7	40.7±13	1.5±0.5	0.91±0.16	2.40±0.50
4	8	3.2±1.8	1.5±0.5	1.64±0.20	2.27±0.10
5	9	43.2±6.0	2.1±0.2	1.01±0.30	2.08±0.10
6	10	38.7±22	2.3±0.5	1.19±0.27	2.08±0.10
7	11	51.4±10	2.3±0.5	1.28±0.20	2.35±0.10
					2.35±0.10
8	12	200±40	1.2±0.3	2.10±0.30	2.20±0.10
9	13	93.4±10	2.0±0.5	2.04±0.40	1.92±0.10
10	13	97.3±10	1.3±0.5	0.98±0.15	2.24±0.10
					1.96±0.20
11	14	133±37	1.5±0.5	0.94±0.18	2.27±0.10
					2.39±0.10
12	15	99.1±46	2.0±0.5	0.95±0.19	2.43±0.10
					2.43±0.14
13	16	222±38	1.3±0.5	0.82±0.23	3.14±0.10
					3.37±0.10
14	17	172±58	1.3±0.5	1.04±0.20	1.80±0.10
					1.88±0.13
15	18	104±50	1.8±0.5	1.17±0.24	2.12±0.14

[a]Average of two methods described in text.

$+ D(Cr_{n-3}^+ - Cr) + D(Cr_{n-2}^+ - Cr) + D(Cr_{n-1}^+ - Cr) + D(O_2)$. Upper limits derived in this manner are listed in Table II. Lower limits to the $Cr_n^+ - (O)_2$ bond energies can be obtained from observations of exothermic reactions. For chromium clusters from $n = 4-11$, the clusters react exothermically with oxygen to form $Cr_{n-3}O_2^+ + 3$ Cr. This is the most probable reaction product at low energies, accounting for nearly 100% of the total cross section at thermal energies. Although concomitant formation of Cr_2 is a lower energy pathway, it is disfavored kinetically for clusters larger than Cr_5^+ as demonstrated in our earlier work on CID of bare chromium cluster cations with Xe.[16] These observations lead to the probable conclusion that $D[Cr_{n-3}^+ - (O)_2 \geqslant D(Cr_{n-3}^+ - Cr) + D(Cr_{n-2}^+ - Cr) + D(Cr_{n-1}^+ - Cr) + D(O_2)$. These lower limits are also listed in Table II.

For larger clusters, the dominant product at low energies becomes $Cr_{n-2}O_2^+$ or $Cr_{n-1}O_2^+$. It is possible that the appearance of these cross sections is controlled not by the thermodynamics but by the lifetimes of these products. Specifically, this possibility considers that loss of three Cr atoms from $Cr_nO_2^+$, $n \geqslant 12$ is still an exothermic process, but the average time required for this dissociation is longer than the 10^{-4} s available experimentally. However, in the case of iron cluster reactions,[11] the shape of the cross sections proved to be a reliable indicator of the thermochemistry and this conclusion is also verified for the chromium cluster reactions below.

2. Direct threshold measurements

Direct measurements of the $Cr_n^+ - (O)_2$ bond energies can be obtained by using Eq. (17) to analyze cross sections for cluster dioxides formed in endothermic processes. For smaller clusters ($n = 6-13$), the cross sections for the $Cr_{n-4}O_2^+$ product were analyzed, and in one case ($n = 7$), that for $Cr_{n-5}O_2^+$ was included. For clusters larger than $n = 12$, cross sections for the $Cr_{n-3}O_2^+$ product were analyzed. The optimized parameters used in Eq. (17) to reproduce the data are listed in Table III and converted to $Cr_{n-x}O_2^+$ thermochemistry by using Eq. (18),

$$D[Cr_{n-x}^+ - (O)_2] = D(Cr_{n-x}^+ - xCr) + D(O_2) - E_0. \quad (18)$$

The bond energies derived from these direct threshold determinations are listed in Table II to allow comparison between values from different systems and with the upper and lower limits established above. In all cases, there is good agreement between the directly measured bond energies and the upper and lower limits derived from inspection of the data.

3. Relative threshold measurements

Another way of obtaining information regarding the cluster dioxides is to examine the energy dependence of the $Cr_{n-x}O_2^+$ clusters formed by sequential loss of Cr atoms. The relative thresholds for these reactions can be measured fairly routinely, thereby bypassing questions regarding internal energies of the reactant clusters. Kinetic shifts should also cancel to a large extent, although there is the possibility that these differences may represent upper limits to the true thermodynamic differences because of different kinetic shifts for subsequent reactions.

Because the shapes of the $Cr_{n-x}O_2^+$ cross sections are similar in their threshold regions, this analysis was accomplished in two simple ways. First, the average energy difference between the cross sections for sequential cluster dioxide products, i.e., $Cr_{n-x}O_2^+$ and $Cr_{n-x-1}O_2^+$, was measured

from semilogarithmic plots of the data like that shown in Figs. 2–6 and Ref. 21. Second, cross section data on linear plots was linearly extrapolated to zero cross section and the difference between the intercepts on the energy axis for sequential cluster dioxide products was taken as the energy difference. In both cases, these energy differences correspond to bond energies for $Cr_{n-1}O_2{}^+-Cr$, and their average are listed in Table III. To compare these values to the $Cr_nO_2{}^+$ thermochemistry obtained above, we convert to $D[Cr_n{}^+-(O)_2]$ using Eq. (19),

$$D[Cr_n{}^+-(O)_2] = D(Cr_{n-1}O_2{}^+-Cr)$$
$$+ D[Cr_{n-1}{}^+-(O)_2]$$
$$- D(Cr_{n-1}{}^+-Cr). \qquad (19)$$

This equation relies on the $Cr_{n-1}{}^+-(O)_2$ bond energies for the next smallest cluster, hence, the values listed in Table II derived from these relative threshold measurements are calculated using the average value for the next smallest cluster. This average is calculated from all available values (those directly measured and the relative values). It can be seen that the agreement between the direct and relative measurements is fairly good, certainly within the experimental error of either determination. The average value listed in Table II is therefore believed to be our best thermochemical information for the cluster dioxides. Further, these average values for n <9 agree with the lower and upper limits determined by loss of three and four chromium atoms being exothermic and endothermic, respectively. For n>10, the average values lie between the lower and upper limits determined by loss of two and three chromium atoms being exothermic and endothermic, respectively. The average value for $n=9$ is an intermediate case such that loss of three chromium atoms (from $Cr_{12}{}^+$) is close to thermoneutral. Thus, the appearance of the cross sections is a good indicator of the endothermicity or exothermicity of the particular process and is not unduly influenced by lifetime effects, in agreement with our conclusions for iron cluster ion reactivity with O_2.[11]

C. Cluster monoxide bond energies, $Cr_n{}^+-O$

1. Qualitative considerations

As a first approximation to the cluster monoxide bond energies, we can assume that the two oxygen bonds in the $Cr_nO_2{}^+$ species are similar, i.e., that $D(Cr_n{}^+-O)$ are approximately half the $D[Cr_n{}^+-(O)_2]$ values listed in Table II. This estimate gives $Cr_n{}^+-O$ bond dissociation energies greater than $D(O_2)$ for all clusters. This means that formation of Cr_nO^+ in reaction (20),

$$Cr_n{}^+ + O_2 \rightarrow Cr_nO^+ + O, \qquad (20)$$

should be exothermic for all clusters. This conclusion contrasts with our observations for all cluster sizes with the exception $n=2$, 4, and 5, that the primary Cr_nO^+ product cross sections appear to have an energy dependence consistent with endothermic processes, Figs. 1–6 and Ref. 21. Although it could have been possible that $D(Cr_n{}^+-O)$ ≪$D(OCr_n{}^+-O)$, this seemed unlikely. To further investigate this matter, we have also studied the reactions of $Cr_n{}^+$

TABLE IV. Summary of parameters used in Eq. (17) for the analysis of $Cr_{m+1}{}^+ + O_2 \rightarrow Cr_mO^+ + Cr + O$ cross sections and calculated bond energies.

m	σ_0	N	E_0, eV	$D(Cr_m{}^+-O)$ (eV)
3	1.1	2.0 (0.3)	1.22 (0.1)	4.94 (0.27)
4	0.17	2.5 (0.3)	0.57 (0.1)	6.78 (0.32)
5	0.18	2.8 (0.3)	0.54 (0.1)	6.34 (0.33)
6	2.0	2.0 (0.3)	1.69 (0.1)	5.98 (0.26)
7	3.2	1.5 (0.3)	1.64 (0.2)	5.73 (0.30)
8	1.2	2.3 (0.3)	1.45 (0.2)	6.25 (0.35)
9	5.7	2.0 (0.3)	1.63 (0.2)	5.89 (0.32)
10	3.0	2.3 (0.3)	1.61 (0.3)	6.08 (0.30)
11	2.5	2.3 (0.3)	1.80 (0.3)	5.98 (0.42)
12	0.27	2.0 (0.4)	2.09 (0.4)	6.03 (0.50)
13	8.7	1.8 (0.3)	1.92 (0.3)	6.25 (0.40)
14	5.1	2.4 (0.3)	2.37 (0.4)	5.52 (0.50)
15	5.9	2.0 (0.3)	2.11 (0.5)	5.93 (0.52)
16	5.7	2.0 (0.3)	2.00 (0.6)	5.95 (0.52)
17	9.6	1.8 (0.5)	2.24 (0.6)	5.04 (0.80)

with carbon dioxide. The thermochemistry determined there, which is reported elsewhere,[13] also indicates that formation of Cr_nO^+ should be exothermic for all chromium clusters n>1.

The Cr_nO^+ are minor products for most cluster sizes and are in direct competition with formation of the cluster dioxides. The competition between losing an oxygen atom from the $Cr_nO_2{}^+$ transient intermediate to form the cluster monoxides in reaction (20) and losing a chromium atom, a much more favorable process energetically, may account for the apparent thresholds observed for the Cr_nO^+ products. It is also possible that there are barriers along the potential energy surface for the oxygen atom loss pathway. In any case, it is clear that the thresholds observed for the $Cr_nO^+ + O$ reaction channel are not reliable measurements of Cr_nO^+ thermochemistry, hence they are not reported in this work.

2. Direct threshold measurements

An alternative method of deriving $Cr_n{}^+-O$ bond energies notes that this bond energy is related to the difference between the thresholds for reactions (21) and (22),

$$Cr_n{}^+ + O_2 \rightarrow Cr_{n-1}{}^+ + Cr + O_2 \qquad (21)$$
$$\rightarrow Cr_{n-1}O^+ + Cr + O. \qquad (22)$$
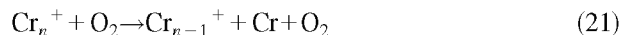
Specifically, the "secondary" bond energies are calculated as $D(Cr_{n-1}{}^+-O) = E_0(21) - E_0(22) + D(O_2)$. The thresholds for reactions (21) are equivalent to the bond energies of the bare chromium cluster ions, $D(Cr_{n-1}{}^+-Cr)$.[16] Here, we determine the thresholds for reactions (22) using an analysis with Eq. (17) as outlined above. The optimized parameters of this model are listed in Table IV, along with the bond dissociation energies of $Cr_n{}^+-O$ obtained from these thresholds using the equation noted above. We also verified that the previously published values of $D_0(Cr_{n-1}{}^+-Cr)$ could be used in Eq. (17) along with reasonable N values to reproduce the present data for reaction (21).

The reliability of these measurements is again hindered by the second order character of these reactions (corresponding to loss of $Cr+O$ from $Cr_nO_2^+$). An additional drawback
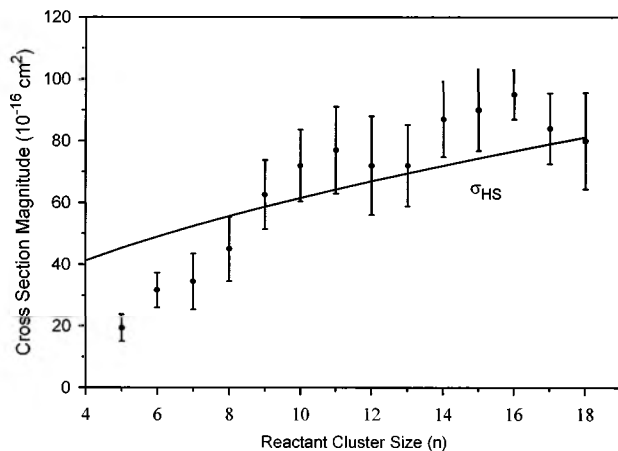
FIG. 7. Comparison of the total reaction cross section of the reactions of Cr_n^+ ($n = 2-18$) with O_2 from the experimental data with the hard sphere limit as a function of cluster size (n). Magnitudes of the total experimental cross sections are averaged over values for energies greater than 0.5 eV.

to measuring thermochemistry in this manner is that the uncertainty is larger because it includes the uncertainties of both reactions (21) and (22). A redeeming feature, however, is that the errors due to the kinetic shifts and internal energies should be reduced because identical assumptions are employed for both threshold measurements.

V. DISCUSSION

A. Efficiency of reactions

For barrierless, exothermic ion–molecule reactions, the Langevin–Gioumousis–Stevenson (LGS) expression can often be used to predict the reaction cross section. Because σ_{LGS} is determined by the polarizability of the neutral gas, it is the same for all cluster ion sizes. Examination of Figs. 1–6 shows that at the very lowest energies, the total reaction cross sections have similar magnitudes and follow an energy dependence that is comparable to $E^{-1/2}$. As the energy is increased, however, the total cross sections begin to plateau to a constant value that is maintained to the highest energies examined. Thus, all of the cluster reactions for $n > 5$ display cross section magnitudes that exceed σ_{LGS} at these slightly elevated energies.

This phenomenon was also observed by Jarrold and Bower in their study of the reactions of aluminum cluster cations with O_2.[28] They reasoned that the predictions of the LGS model failed because the physical size of the cluster exceeds σ_{LGS} at even modest kinetic energies. Figure 7 shows the average cross section magnitudes measured experimentally at energies above 0.5 eV along with 30% uncertainties. For clusters larger than $n = 5$, the cross section magnitudes change little above 0.5 eV, while for smaller clusters, there is more variation with energy. Indeed, for Cr_n^+ ($n = 3$ and 4), the energy dependence follows the LGS prediction throughout the energy ranges examined and hence these magnitudes are not included in Fig. 7. For $n = 5$, the total cross section deviates from σ_{LGS} only above 5 eV and this limiting value is shown in Fig. 7. These experimental cross sections are compared in Fig. 7 with a hard sphere

cross section limit calculated as $\sigma_{HS} = \pi d^2$ where d is the cluster radius plus the dioxygen radius. The radius of the cluster was estimated using the packing pattern of the body centered cubic crystal and the assumption that the cluster is spherical. With the exception of the smallest clusters and a few outliers, this comparison demonstrates that the reactions occur with unit efficiency that is largely controlled by the size of the cluster. This conclusion is identical to that reached by Nieman and co-workers for the reactions of neutral chromium clusters with O_2 in a flow tube reactor.[8]

B. Reaction mechanism

The mechanism for the reactions of chromium cluster ions with O_2 appears fairly straightforward. Dissociative chemisorption of the O_2 molecule on the cluster surface heats the cluster strongly (by 4 to 7 eV based on the thermochemistry in Table II) and dissociation ensues. Because chromium–oxygen bonds are stronger than chromium–chromium bonds, this dissociation is dominated by chromium atom loss to form cluster dioxide ions. Oxygen atom loss to form cluster monoxide ions is much less efficient. As noted above, competition between these two channels appears to occur early in the reaction scheme, indicating that oxygen atom loss occurs primarily from the transient $Cr_nO_2^+$ intermediate. This seems reasonable as dissociation cools the remaining cluster such that subsequent dissociations must occur primarily along the lowest energy pathways available. It is possible that kinetic factors that inhibit facile rearrangements of the metal clusters needed to accommodate the oxygen atoms may facilitate the oxygen atom loss channel. In addition to atomic loss processes, loss of molecular products such as CrO and Cr_2O can also occur; as discussed further below. As the kinetic energy of the reactants is increased, the primary products dissociate further with loss of atomic chromium again being the most prominent dissociation process. Additional minor products observed are the cluster fragments, which result primarily from direct CID for all clusters larger than Cr_6^+. These are inefficient reactions that presumably occur upon those rare occasions when the orientation of the $Cr_n^+ + O_2$ reactants leads to a more impulsive collision.

C. Trends in oxygenated chromium cluster stabilities

The various chromium cluster–oxygen bond energies derived above are shown as a function of cluster size in Fig. 8. It can be seen that the cluster oxygen bond energies do not vary strongly with cluster size above $n = 3$. It can also be seen that the $Cr_n^+ - O$ bond energies derived from the secondary Cr_nO^+ product thresholds agree fairly well with half the $Cr_n^+ - (O)_2$ bond energies, although the $Cr_n^+ - O$ bond energies are systematically lower for clusters larger than $n = 5$. In addition, these bond energies are systematically lower than those derived from our accompanying study with CO_2,[13] although within the combined experimental errors in all but a few cases. We believe that these slightly lower bond energies are probably the result of thresholds for formation of $Cr_{n-1}O^+$ shifted to higher energies by competition with the cluster dioxide products.
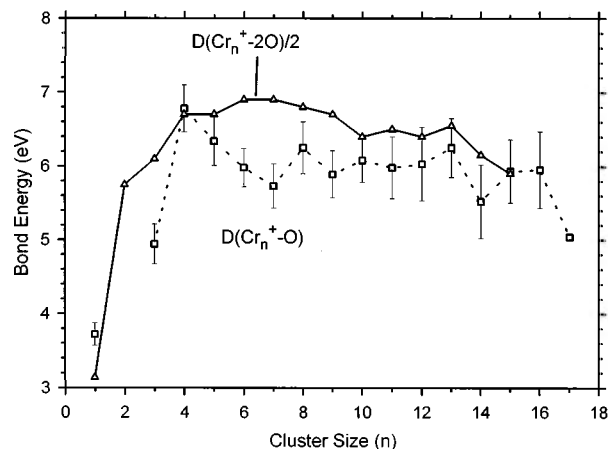
FIG. 8. Comparison of the cluster monoxide and dioxide bond energies from this study.

FIG. 9. Comparison of $D(O_xCr_{n-1}{}^+-Cr)$ for $x=1$ and 2 calculated using Eq. (23) and $D(OCr_{n-1}{}^+-CrO)/2$ calculated using Eq. (24) to the CID bond energies, as a function of the total number of chromium atoms in the cluster (n).

Another way to examine the trends in this thermochemistry is to compare the stabilities of bare and oxygenated cluster ions with regard to loss of a chromium atom, the lowest energy dissociation process in all cases. These $O_xCr_{n-1}{}^+-Cr$ bond energies where $x=1$ and 2 are calculated from Eq. (23),

$$D(O_xCr_{n-1}{}^+-Cr) = D[Cr_n{}^+-(O)_x]$$
$$-D[Cr_{n-1}{}^+-(O)_x]$$
$$+D(Cr_{n-1}{}^+-Cr), \qquad (23)$$

where the required bond energies are taken from Table II, Ref. 16, and $D(Cr_n{}^+-O)$ are from Ref. 13. These comparisons are shown in Fig. 9. For most cluster sizes, Fig. 9, the pattern in dissociation energies, $D(O_xCr_{n-1}{}^+-Cr)$ differs from that for bare clusters, $D(Cr_{n-1}{}^+-Cr)$. The strong even–odd alternation observed in the bond energies of the bare clusters is suppressed in the mono-oxygenated and di-oxygenated species. The lack of large changes in the bond energies upon oxygenation simply reflects the fact that the $Cr_n{}^+-(O)_2$ and $Cr_n{}^+-O$ bond energies do not change appreciably with cluster size, Fig. 8, except for the smallest clusters. The most dramatic effect of oxygenating the clusters is to stabilize the smallest even-sized clusters, $Cr_2{}^+$ $Cr_4{}^+$, and $Cr_6{}^+$. It is believed that these clusters are less stable than their neighbors because they involve an odd number of $4s$ electrons in the bonding while the odd-sized clusters can pair all $4s$ electrons. It seems plausible that oxygenation enhances the stability of these clusters by bonding in bridging sites and tying up unpaired electrons on the metal atoms.

Another comparison can be made by calculating the energy required to remove a CrO neutral from the dioxygenated cluster using Eq. (24),

$$D(OCr_{n-1}{}^+-CrO) = D[Cr_n{}^+-(O)_2] - D[Cr_{n-1}{}^+-O]$$
$$+D(Cr_{n-1}{}^+-Cr) - D(CrO), \qquad (24)$$

where the required bond energies are taken from Tables II and IV, Ref. 16, and $D(Cr_2{}^+-O)$ is from Ref. 13. The results of this calculation are also plotted in Fig. 9 (the result is
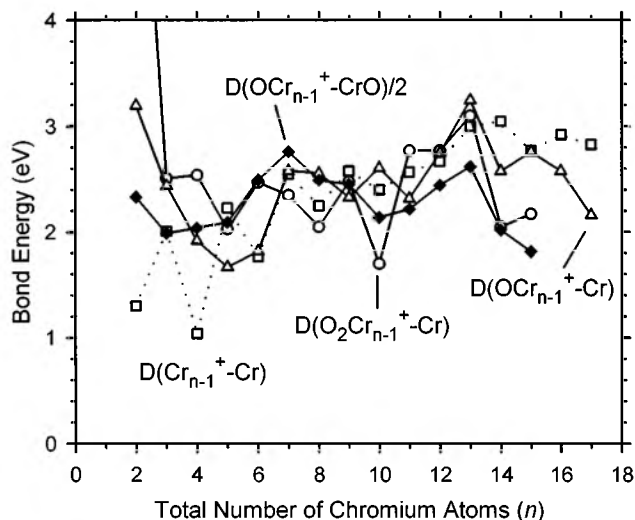
divided by two to fit the scale of the figure). This process requires an average of about 5 eV for the larger clusters, therefore, it is understandable that metal evaporation is the most efficient cooling mechanism.

D. Comparison to oxidation of neutral chromium clusters

Nieman et al. performed flow tube reactor studies on the oxidation of transition metal clusters.[8] They observed that during the initial stages of oxidation, the cluster dioxide products were the first peaks to increase in the mass spectrum. This is consistent with our observation that the cluster dioxide products dominate the spectrum at thermal energies for all but the smallest clusters. They reasoned that the more exothermic addition of O_2 predominates over the approximately thermoneutral addition of a single O atom, as quantified directly here. They also stated that an important cooling mechanism for the oxygenated clusters is by evaporation, as observed directly in the present study.

E. Comparison to bulk phase thermochemistry

Ideally, we would like to compare the bond energies determined here to those on bulk phase Cr surfaces. While there have been several experimental studies on the oxidation on both polycrystalline and single crystal Cr surfaces, the results reported are mostly qualitative.[9] The analysis of this work on single crystal surfaces is complicated by the observation that oxidation induces the metal atoms to migrate and the surface to reorganize. The most current thermodynamic measurements come from calorimetry experiments that give 7.6 ± 0.3 eV for the desorption of O_2 from chromium films.[10] This is equivalent to $Cr_n{}^+-(O)_2$ bond energies of 12.7 ± 0.3 eV ($=7.6+5.1$), comparable to the 11.5–13.8 eV range found here (Table II). In addition, $\Delta_{vap}H^0$ (Cr) is 4.10 ± 0.04 eV, suggesting that the metal should vaporize before oxygen desorbs for many oxidized chromium surfaces. The adsorption of molecular oxygen on chromium surfaces has been shown to undergo a dissociative

chemisorption mechanism. Using the heat of adsorption value given above, this leads to a metal surface–oxygen bond energy in the range 6.4±0.2 eV. It is interesting that most of our measurements for the Cr_nO^+ bond energies and half the $Cr_nO_2^+$ bond energies fall in the range of 5–7 eV for clusters $n > 1$ and the average for clusters in this range is 6.43±0.44 eV. Thus, the thermochemistry obtained here for small chromium clusters is comparable to that for bulk phase chromium. Further, the average of the iron oxide cluster bond energies (Fe_n^+–O and half the Fe_n^+–O_2 values) is 5.5±0.5 eV.[11,12] This difference in cluster properties clearly reflects the driving force for the selective oxidation of chromium in Fe–Cr alloys. This suggests that the use of clusters to model the reactivity at surface defects, at least for oxygen, may be reasonable.[33]

ACKNOWLEDGMENT

[1] F. P. Fehlner and M. J. Graham, in *Corrosion Mechanisms in Theory and Practice*, edited by P. Marcus and J. Odar (Marcel Dekker, New York, 1995), p. 136.

[2] E. R. Fisher, J. L. Elkind, D. E. Clemmer, R. Georgiadis, S. K. Loh, N. Aristov, L. S. Sunderlin, and P. B. Armentrout, J. Chem. Phys. **93**, 2676 (1990).

[3] D. L. Hildenbrand, Chem. Phys. Lett. **34**, 352 (1975).

[4] P. G. Wenthold, R. F. Gunnion, and W. C. Lineberger, Chem. Phys. Lett. **258**, 101 (1996).

[5] A. Hachimi, E. Poitevin, G. Krier, J. F. Muller, and M. F. Ruiz-Lopez, Int. J. Mass Spectrom. Ion Processes **144**, 23 (1995), and references therein.

[6] J. M. Dyke, B. J. W. Gravenor, R. A. Lewis, and A. Morris, J. Chem. Soc., Faraday Trans. 2 **79**, 1083 (1983).

[7] G. V. Chertihin, W. D. Bare, and L. Andrews, J. Chem. Phys. **107**, 2798 (1997), and references therein.

[8] G. C. Nieman, E. K. Parks, S. C. Richtsmeier, K. Liu, L. G. Pobo, and S. J. Riley, High. Temp. Sci. **22**, 115 (1986).

[9] L. Zhang, M. Kuhn, and U. Diebold, Surf. Sci. **375**, 1 (1997); A. Stierle, P. Bödecker, and H. Zabel, *ibid.* **327**, 9 (1995); N. M. D. Brown and H.-X. You, *ibid.* **233**, 317 (1990); U. S. Foord and R. M. Lambert, *ibid.* **161**, 513 (1985); F. Watari and J. M. Cowley, *ibid.* **105**, 240 (1981); C. Gewinner, J. C. Peruchetti, A. Jaegle, and A Kalt, *ibid.* **78**, 439 (1978); S. Ekelund and C. Leygraf, *ibid.* **40**, 179 (1973).

[10] D. Brennan, D. O. Hayward, and B. M. W. Tradnell, Proc. R. Soc. London, Ser. A **256**, 81 (1960); J. Bragg and F. C. Tomkins, Trans. Faraday Soc. **51**, 1071 (1955); G. Wedler, Z. Phys. Chem. **27**, 388 (1961).

[11] J. B. Griffin and P. B. Armentrout, J. Chem. Phys. **106**, 4448 (1997).

[12] J. B. Griffin and P. B. Armentrout, J. Chem. Phys. **107**, 5345 (1997).

[13] J. B. Griffin and P. B. Armentrout, J. Chem. Phys. **108**, 8075 (1998), following paper.

[14] J. Xu, M. T. Rodgers, J. B. Griffin, and P. B. Armentrout, J. Chem. Phys. (to be published).

[15] J. Conceição, S. K. Loh, L. Lian, and P. B. Armentrout, J. Chem. Phys. **104**, 3976 (1996).

[16] C.-X. Su and P. B. Armentrout, J. Chem. Phys. **99**, 6506 (1993).

[17] S. K. Loh, L. Lian, and P. B. Armentrout, J. Chem. Phys. **91**, 6148 (1989).

[18] E. Teloy and D. Gerlich, Chem. Phys. **4**, 417 (1974); D. Gerlich, Adv. Chem. Phys. **82**, 1 (1992).

[19] N. R. Daly, Rev. Sci. Instrum. **31**, 264 (1959).

[20] K. M. Ervin and P. B. Armentrout, J. Chem. Phys. **83**, 166 (1985).

[21] See AIP Document No. PAPS JCPSA6-108-019819 for 32 pages of figures. Order by PAPS number and journal reference from American Institute of Physics, Physics Auxiliary Publication Service, Carolyn Gehlbach, 500 Sunnyside Boulevard, Woodbury, New York 11797-2999. Fax: 516-576-2223, e-mail: paps@aip.org. The price is $1.50 for each microfiche (98 pages) or $5.00 for photocopies of up to 30 pages, and $0.15 for each additional page over 30 pages. Airmail additional. Make checks payable to the American Institute of Physics.

[22] M. W. Chase, C. A. Davies, J. R. Downey, D. J. Frurip, R. A. McDonald, and A. N. Syverud, J. Chem. Phys. **14**, Suppl. 1 (JANAF) (1985).

[23] G. Gioumousis and D. P. Stevens, J. Chem. Phys. **29**, 294 (1958).

[24] E. W. Rothe and R. B. Bernstein, J. Chem. Phys. **31**, 1619 (1959).

[25] J. Sugar and C. Corliss, J. Phys. Chem. Ref. Data **14**, Suppl. 2 (1985).

[26] R. T. Grimley, R. P. Burns, and M. G. Inghram, J. Chem. Phys. **34**, 664 (1961).

[27] P. B. Armentrout, in *Advances in Gas Phase Ion Chemistry*, edited by N. G. Adams and L. M. Babcock (JAI, Greenwich, 1992), Vol. I, pp. 83–119.

[28] M. F. Jarrold and J. E. Bower, J. Chem. Phys. **87**, 5728 (1987).

[29] J. L. Elkind and P. B. Armentrout, J. Am. Chem. Soc. **90**, 6576 (1986); P. B. Armentrout, Int. Rev. Phys. Chem. **9**, 115 (1990); D. E. Clemmer, Y.-M. Chen, N. Aristov, and P. B. Armentrout, J. Chem. Phys. **98**, 7538 (1994).

[30] K. M. Ervin and P. B. Armentrout, J. Chem. Phys. **83**, 166 (1985).

[31] M. E. Weber, J. L. Elkind, and P. B. Armentrout, J. Chem. Phys. **84**, 1521 (1986).

[32] M. T. Rodgers, K. M. Ervin, and P. B. Armentrout, J. Chem. Phys. **106**, 4499 (1997).

[33] G. Somorjai, *Chemistry in Two Dimensions: Surfaces* (Cornell University Press, Ithaca, 1981).

[34] C.-X. Su, D. A. Hales, and P. B. Armentrout, Chem. Phys. Lett. **201**, 199 (1993).

[35] P. B. Armentrout, L. F. Halle and J. L. Beauchamp, J. Chem. Phys. **76**, 2449 (1982).